DISCOVERING FIBONACCI NUMBERS, FIBONACCI WORDS, AND A FIBONACCI FRACTAL IN THE TOWER OF HANOI

ANDREAS M. HINZ AND PAUL K. STOCKMEYER

Abstract. The Tower of Hanoi puzzle, with three pegs and n graduated discs, was invented by Édouard Lucas in 1883, writing under the name of Professor Claus. A simple question about relative distances between various regular states of this puzzle has lead to the discovery of a new occurrence of Fibonacci numbers, a new illustration of the finite Fibonacci words, and a fractal of Hausdorff dimension $\log_2(\phi)$, where ϕ is the Golden ratio.

1. Introduction and Background

The Tower of Hanoi, a puzzle invented in 1883 by French mathematician Édouard Lucas writing under the *nom de plume* Professor Claus [3, 4], consists of three vertical pegs and n discs of mutually different diameters. The discs are pierced in the center so that they can be stacked on the pegs. Following [7], any stacking of the discs on the pegs with no larger disc lying on a smaller one is called a *regular state* of the puzzle. A regular state in which all the discs are stacked on a single peg is called a *perfect state*. The pegs are labeled 0, 1, and 2, and the discs are labeled from 1 to n in increasing order of diameter. A *legal move* consists of moving a disc from the top of one stack to the top of a (possibly empty) stack on another peg, but never placing a disc on top of a smaller one. The classical task is to transform an initial perfect state into a final perfect state through a minimum-length sequence of legal moves. It is well known that there exists a unique such sequence, consisting of 2^n-1 moves. For more information about the Tower of Hanoi, see the comprehensive book [7] by Hinz, Klavžar, and Petr.

The *Fibonacci numbers* F_k, familiar to all readers of this journal, are defined by $F_0 = 0$, $F_1 = 1$, and $F_n = F_{n-1} + F_{n-2}$ for $n \geq 2$. Perhaps less familiar are the (finite) *Fibonacci words* W_k, strings of the symbols 0 and 1, discussed thoroughly by Allouche and Shallit in [1, Chapter 7]. We give two characterizations of these words.

Characterization 1: The Fibonacci words W_k can be defined by

- $W_0 = 1$;
- $W_1 = 0$; and
- $W_n = W_{n-1}W_{n-2}$ for $n \geq 2$,

the concatenation of previously defined words.

Characterization 2: The Fibonacci words W_k can be defined by

- $W_0 = 1$; and
- $W_{n+1} = \varphi(W_n)$,

where φ is the *Fibonacci morphism* defined by $\varphi(0) = 01$ and $\varphi(1) = 0$. The proof that these two characterizations agree can be found, for example, in [1, Theorem 7.1.1]. These two characterizations will provide us with dual presentations of some of the concepts discussed in Sections 4 and 5.

The first nine finite Fibonacci words are displayed in Table 1. Note that the word W_n

$$
\begin{aligned}
W_0 &= 1\\
W_1 &= 0\\
W_2 &= 01\\
W_3 &= 010\\
W_4 &= 01001\\
W_5 &= 01001010\\
W_6 &= 0100101001001\\
W_7 &= 010010100100101001010\\
W_8 &= 0100101001001010010100100101001001
\end{aligned}
$$

Table 1. The first nine finite Fibonacci words.

consists of F_n copies of the symbol 0 and F_{n-1} copies of the symbol 1, for a total length of F_{n+1} symbols. As n increases, these words approach the infinite Fibonacci word; see sequence A003849 in [8].

There is a known result linking the Tower of Hanoi puzzle with the Fibonacci numbers. Bennish [2] reports that the number of different legal arrangements of discs on the initial, intermediate, and final pegs encountered in the optimal move sequence for the classical Tower of Hanoi puzzle are the Fibonacci numbers F_{n+2}, F_{n+1}, and F_{n+2}, respectively (cf. [7, Exercise 2.6] and its solution). He attributes this result to his colleague Kent Merryfield. In this paper we present a new link between these two classics of recreational mathematics, as well as a link between the Tower of Hanoi and the finite Fibonacci words.

2. Distances in the Hanoi Graphs H_3^n

A great deal of insight can be gained by examining the Hanoi graph H_3^n for the puzzle with n discs and 3 pegs. The vertices of this graph are the 3^n regular states of the puzzle. Each state is represented by the sequence $s_n s_{n-1} \dots s_1 \in T^n$, where $T = \{0, 1, 2\}$ and s_i denotes the peg containing disc i. Two vertices are adjacent if one can be reached from the other by a legal move of one disc. These graphs are easily seen to be connected and planar, and are customarily drawn on and inside an equilateral triangle, with all edges having the same length. We follow the convention of placing the perfect state 0^n at the center top point, with coordinates $\left(\frac{1}{2}, \frac{\sqrt{3}}{2}\right)$, the perfect state 1^n in the lower left corner point, with coordinates $(0, 0)$, and the perfect state 2^n in the lower right corner point, with coordinates $(1, 0)$. Figure 1 shows the standard display of the graph H_3^5 with the perfect states labeled.

We define the distance $d(v_1, v_2)$ between vertices v_1 and v_2 in H_3^n to be the number of edges in a minimal-length path from v_1 to v_2. (Alternatively, $d(v_1, v_2)$ is the minimum number of disc moves required to transform the Tower of Hanoi state corresponding to v_1 into the state corresponding to v_2.) We are particularly interested in the distances from an arbitrary vertex v to the perfect vertices 0^n, 1^n, and 2^n, and for each $i \in T$ we use the abbreviation $d_i(v)$ for $d(v, i^n)$.

The following facts are well known. See, for example, [7, Theorem 2.7, Lemma 2.8, and Proposition 2.13].

Facts:

(1) We have $0 \le d_i(v) \le 2^n - 1$ for all v in H_3^n and all $i \in \{0, 1, 2\}$.

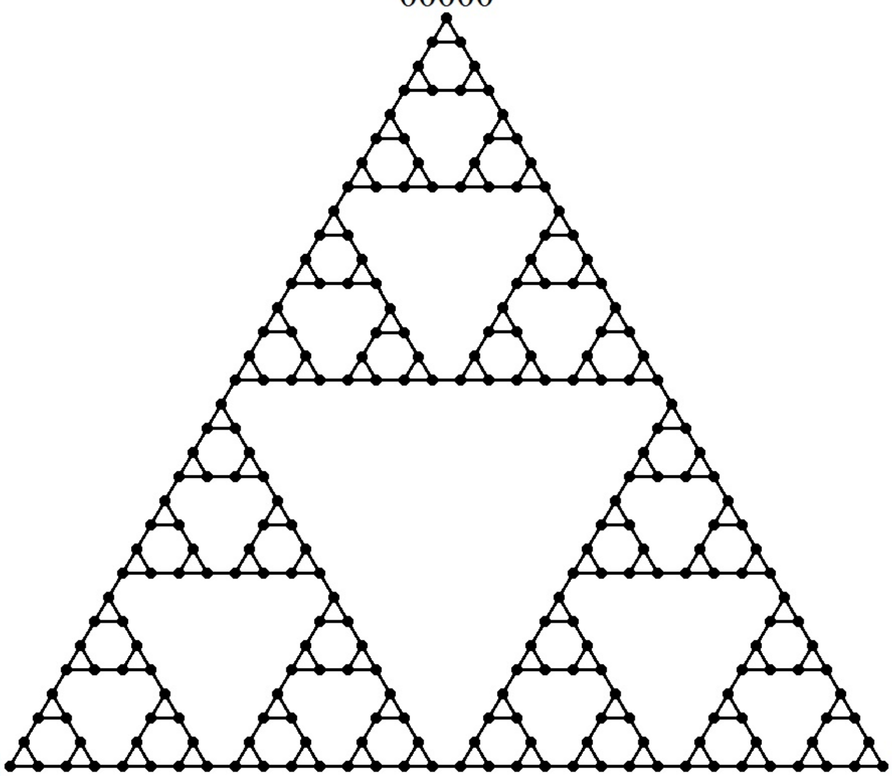

FIGURE 1. Drawing of the graph H_3^5.

(2) Every vertex v of H_3^n is uniquely determined by the three distances $d_0(v)$, $d_1(v)$, and $d_2(v)$.
(3) For any v in H_3^n we have $d_0(v) + d_1(v) + d_3(v) = 2\,(2^n - 1)$.

Note that by combining (2) and (3) above, we conclude that every vertex v is uniquely determined by any two of the distances $d_0(v)$, $d_1(v)$, and $d_2(v)$ ([7, Remark 2.14]).

In view of these facts, it is natural to ask for a rule determining, given three numbers d_0, d_1, and d_2, when there exists a vertex v of H_3^n with $d_0(v) = d_0$, $d_1(v) = d_1$, and $d_2(v) = d_2$. Properties (1) and (3) above, while necessary, are not sufficient. For example, with $n = 2$, the values $d_0 = d_1 = d_2 = 2$ satisfy these properties, but there is no vertex v of H_3^2 with these distances.

Theorem 2.1. *For any three nonnegative integers d_0, d_1, and d_2, each at most $2^n - 1$, there exists a vertex v of H_3^n with these distances to the three perfect vertices if and only if for each of the n bit positions in the binary representations of these three integers, exactly one of the three numbers has a 0 in that bit position.*

Proof. The proof, by induction on n, follows that of Lemma 2.8 in [7]. The graph H_3^1 is in fact the complete graph K_3, with distances 0, 1, and 1, so the claim is true in this case. We suppose that the claim is true in the graph H_3^n for some arbitrary n. Consider an arbitrary vertex $v = it$ in the graph H_3^{n+1}, where $i \in T$ and $t \in T^n$. Then

$$d(v, i^{n+1}) = d(it, i^{n+1}) = d(t, i^n) \leq 2^n - 1,$$

while for $j \in T, j \neq i$ we have

$$d(v, j^{n+1}) = d(it, j^{n+1}) = d(t, (3-i-j)^n) + 2^n \geq 2^n.$$

Thus the left-most bit of $d_i(v)$ is 0 while for $j \neq i$ the left-most bit of $d_j(v)$ is 1. The remaining bits come from the three distances $d(t, i^n)$, $d(t, j^n)$ and $d(t, k^n)$, which by the induction hypothesis must have the desired bit property.

Conversely, consider three nonnegative distances d_0, d_1, and d_2, each at most $2^{n+1} - 1$, satisfying the bit property of the theorem. If d_i is the unique distance with 0 as its leftmost bit, we know that any vertex with these distances must be of the form it for some $t \in T^n$. The induction hypothesis guarantees the existence of a vertex $v' = s' \in T^n$ with distance d_i to vertex i^n, distance $d_j - 2^n$ to vertex $(3-i-j)^n$, and distance $d_k - 2^n$ to vertex $(3-i-k)^n$. Then $v = is'$ is the desired vertex in H_3^{n+1}. □

Example: For $n = 6$, consider the distances $d_0 = 29$, $d_1 = 39$, and $d_2 = 58$. We have

$$\begin{aligned} d_0 &= 29 = (011101)_{(2)} \\ d_1 &= 39 = (100111)_{(2)} \\ d_2 &= 58 = (111010)_{(2)} \end{aligned}$$

so yes, there is such a vertex v. Each column of the binary representations contains exactly one 0.

Theorem 2.1 is not only useful in what follows, it is also reassuring. It provides additional confirmation that the number of vertices in H_3^n is 3^n and that $d_1 + d_2 + d_3 = 2(2^n - 1)$.

3. The Key Results

Our main result answers a seemingly innocent question. We say a vertex v is a *key* vertex of H_3^n if $d_2(v) = 2d_0(v)$, and ask for the number of key vertices in the graph H_3^n. Figure 2, showing the key vertices in the graph H_3^6, hints at the remarkable answer. We see that there are five key vertices, and that they partition naturally into three on the left and two on the right. Moreover, the three on the left partition into two and one. With this hint, our next result is not surprising.

Theorem 3.1. *The number of key vertices of graph H_3^n is the Fibonacci number F_{n-1}.*

In the proof of this theorem we will make use of the following lemma.

Lemma 3.2. *A number d_0 is a valid value of $d_0(v)$ for a key vertex v of H_3^n if and only if in the n-bit binary representation of d_0,*

(1) *the left-most bit is 0;*
(2) *the right-most bit is 1; and*
(3) *there are no two consecutive 0 bits.*

Proof of Lemma 3.2. For any vertex v of H_3^n we write its three distances in binary as

$$\begin{aligned} d_0(v) &= (d_{0,n-1}\, d_{0,n-2}\, \ldots\, d_{0,1}\, d_{0,0})_{(2)}\,, \\ d_1(v) &= (d_{1,n-1}\, d_{1,n-2}\, \ldots\, d_{1,1}\, d_{1,0})_{(2)}, \text{ and} \\ d_2(v) &= (d_{2,n-1}\, d_{2,n-2}\, \ldots\, d_{2,1}\, d_{2,0})_{(2)}. \end{aligned}$$

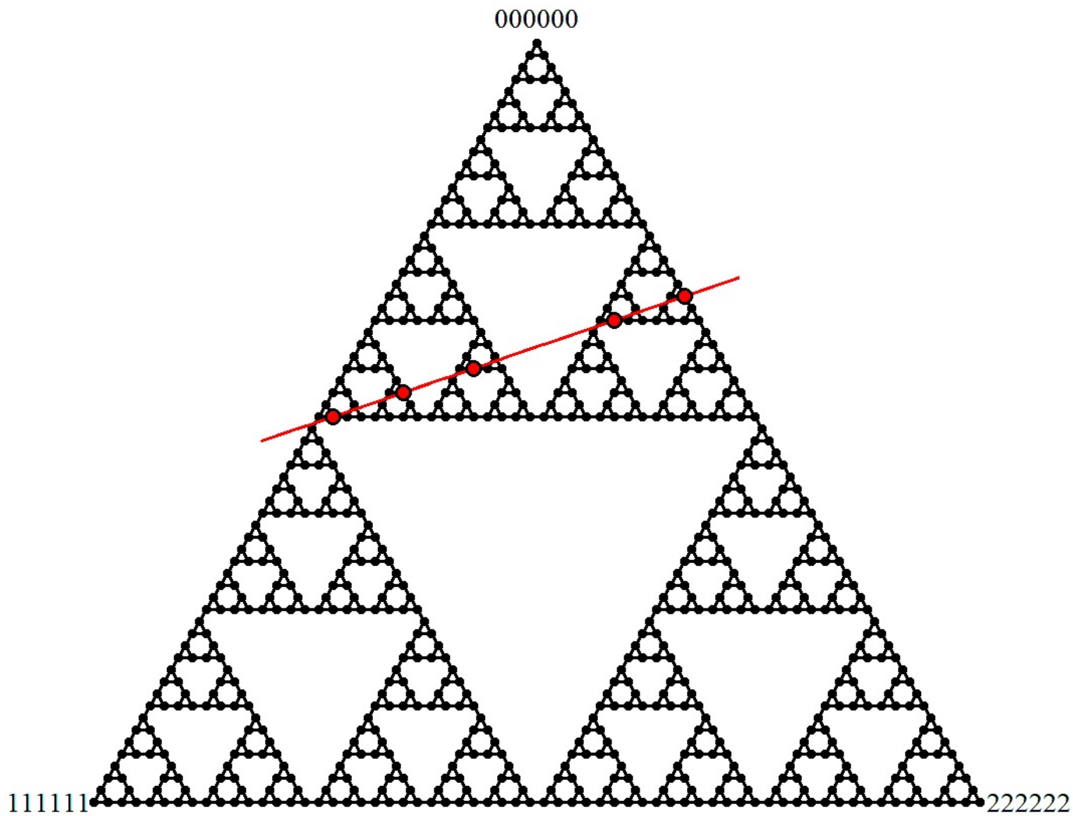

FIGURE 2. Key vertices in H_3^6.

If v is a key vertex, then $2d_0(v) = d_2(v) < 2^n$, or $d_0(v) < 2^{n-1}$, making $d_{0,n-1} = 0$. Also, $d_2(v)$ being even makes $d_{2,0} = 0$, and Theorem 2.1 then forces $d_{0,0} = 1$. Moreover, Theorem 2.1 prohibits $d_{0,i}$ and $d_{2,i}$ both being 0 for $1 \leq i \leq n-1$. But $d_{2,i} = d_{0,i-1}$ for key vertices, so $d_{0,i}$ and $d_{0,i-1}$ cannot both be 0.

Conversely, suppose an n-bit number d_0 has the properties listed. We define d_2 by $d_2 = 2d_0$, and observe that $d_{0,i}$ and $d_{2,i}$ are not both 0, for $0 \leq i \leq n-1$. The distance d_1 is defined by $d_{1,i} = 2 - d_{0,i} - d_{2,i}$ for $0 \leq i \leq n-1$. Then d_0, d_1, and d_2 satisfy the requirements of Theorem 2.1 for the existence of a vertex v with these distances. □

Table 2 lists the three distances for each of the five key vertices of H_3^6 illustrated in Figure 2. The reader can easily verify that for each vertex v_i we have $d_2(v_i) = 2d_0(v_i)$, and both Lemma 3.2 and Theorem 2.1 are satisfied.

Proof of Theorem 3.1. The proof is by induction. Clearly a key vertex v of H_3^n is uniquely determined by the value $d_0(v)$. For $n = 1$ there is no number d_0 satisfying Lemma 3.2 so the number of key vertices is $F_0 = 0$. For $n = 2$ the unique value for d_0 satisfying Lemma 3.2 is $d_0 = 1 = (01)_{(2)}$, leading to $d_2 = 2 = (10)_{(2)}$ and $d_1 = 3 = (11)_{(2)}$. Thus the number of key vertices of H_3^2 is $F_1 = 1$. Similarly, for $n = 3$ we have $d_0 = 3 = (011)_{(2)}$, $d_2 = 6 = (110)_{(2)}$, $d_1 = 5 = (101)_{(2)}$ and therefore exactly $F_2 = 1$ key vertex in H_3^3.

$d_0(v_1) = 31 = (011111)_{(2)}$	$d_0(v_2) = 29 = (011101)_{(2)}$	$d_0(v_3) = 27 = (011011)_{(2)}$
$d_1(v_1) = 33 = (100001)_{(2)}$	$d_1(v_2) = 39 = (100111)_{(2)}$	$d_1(v_3) = 45 = (101101)_{(2)}$
$d_2(v_1) = 62 = (111110)_{(2)}$	$d_2(v_2) = 58 = (111010)_{(2)}$	$d_2(v_3) = 54 = (110110)_{(2)}$

$d_0(v_4) = 23 = (010111)_{(2)}$	$d_0(v_5) = 21 = (010101(_{(2)}$
$d_1(v_4) = 57 = (111001)_{(2)}$	$d_1(v_5) = 63 = (111111)_{(2)}$
$d_2(v_4) = 46 = (101110)_{(2)}$	$d_2(v_5) = 42 = (101010)_{(2)}$

Table 2. The distances for the five key vertices of H_3^6.

Now let n be an arbitrary integer greater than 3, and assume the claim is true for all smaller values. We partition the set of key vertices of H_3^n into two classes. Class 1 consists of key vertices whose d_0 values start out $d_0(v) = (011\ldots)_{(2)}$, while Class 2 consists of key vertices whose d_0 values start out $d_0(v) = (0101\ldots)_{(2)}$. For each vertex v in Class 1 we can delete the leftmost 1 in the binary representation of $d_0(v)$, in effect subtracting 2^{n-2}, to obtain a valid d_0 value for a key vertex of H_3^{n-1}. Moreover, we can reverse this process by adding 2^{n-2} to the d_0 value of any key vertex of H_3^{n-1} to obtain a valid d_0 value of a key vertex of H_3^n. Thus there exist F_{n-2} key vertices of Class 1 in H_3^n.

Similarly, for each vertex v in Class 2 we can delete the leftmost 10 substring in the binary representation of $d_0(v)$, in effect again subtracting 2^{n-2}, to obtain a valid d_0 value for a key vertex of H_3^{n-2}. Moreover, we can reverse this process by adding 2^{n-2} to the d_0 value of any key vertex of H_3^{n-2} to obtain a valid d_0 value of a key vertex of H_3^n. Thus there exist F_{n-3} key vertices of Class 1 in H_3^n for a total of $F_{n-2} + F_{n-3} = F_{n-1}$ key vertices of H_3^n. In fact, the d_0 values of all key vertices of H_3^n can be obtained by adding 2^{n-2} to the d_0 values of the key vertices of H_3^{n-1} and H_3^{n-2}. $\square$

Of the five key vertices of H_3^6 listed in Table 2, the first three are in Class 1 and appear in the left half of Figure 2. The final two are in Class 2, and appear in the right half of the figure. We observe that for all key vertices v of H_3^n we have $2^{n-2} \le d_0(v) < 2^{n-1}$, so there is no overlap between d_0 values of key vertices of graphs of different orders. The sequence of all possible d_0 values for key vertices starts out 1, 3, 5, 7, 11, 13, 15, 21, 23, 27, 29, 31, 43, 45, 47, 53, 55, 59, 61, 63, ... It is sequence A247648 in the OEIS [8].

Figure 2 illustrates another vital fact about key vertices.

Theorem 3.3. *A vertex of graph H_3^n is a key vertex if and only if it lies on the line joining the point $A = \left(\frac{1}{4}, \frac{\sqrt{3}}{4}\right)$ half-way up the left side of the graph with the point $B = \left(\frac{2}{3}, \frac{\sqrt{3}}{3}\right)$ two-thirds of the way up the right side of the graph when the graph is drawn in standard position.*

Proof. The vertices of H_3^n that are d_0 steps from vertex 0^n, for $0 \le d_0 \le 2^n - 1$, all lie along the horizontal line

$$L_0: \qquad y = \frac{\sqrt{3}}{2}\left(1 - \frac{d_0}{2^n - 1}\right),$$

while the vertices that are d_2 steps from vertex 2^n all lie along the line

$$L_2: \qquad y = \sqrt{3}\left(x - 1 + \frac{d_2}{2^n - 1}\right)$$

with slope $\sqrt{3}$. These two lines intersect for

$$x = \frac{1}{2}\left(3 - \frac{d_0 + 2d_2}{2^n - 1}\right) = \frac{1}{2}\left(3 - \frac{5d_0}{2^n - 1}\right),$$

the latter for $d_2 = 2d_0$. With this formula, together with the formula for y from L_0, we have parametric equations for the *magic line* ML containing all points that are twice as far from vertex 2^n as from vertex 0^n. We can eliminate the parameter d_0 to obtain the form

$$ML: \qquad y = \frac{\sqrt{3}}{5}(x+1).$$

This line passes through points A and B with slope $\frac{\sqrt{3}}{5}$. Clearly a vertex is key if and only if it lies on this line. □

Point A is not a vertex of H_3^n, but the leftmost key vertex v_L of H_3^n, with distances $d_0 = 2^{n-1} - 1$, $d_1 = 2^{n-1} + 1$, and $d_2 = 2^n - 2$ is close by and approaches point A in the limit as n increases. When n is even, point B is in fact the rightmost key vertex v_{R1}, with distances $d_0 = \frac{1}{3}(2^n - 1)$, $d_1 = 2^n - 1$, and $d_2 = \frac{2}{3}(2^n - 1)$. When n is odd, point B is not a vertex of H_3^n but the rightmost key vertex v_{R2}, with distances $d_0 = \frac{1}{3}(2^n + 1)$, $d_1 = 2^n - 3$, and $d_2 = \frac{2}{3}(2^n + 1)$, is close by and approaches point B as a limit as n increases. Thus for $n \geq 4$ the magic line could also be described as the line connecting vertex v_L with v_{R1} (n even) or v_{R2} (n odd).

4. Magic Lines and the Sierpiński Triangle

It is well known that, when properly embedded and scaled, the graphs H_3^n approach a fractal, often called the *Sierpiński gasket* or the *Sierpiński triangle* (ST). See, for example, [7, page 151]. A common way to construct this fractal is to start with set ST_0, a filled equilateral triangle with vertices $v_0 = \left(\frac{1}{2}, \frac{\sqrt{3}}{2}\right)$, $v_1 = (0,0)$, and $v_2 = (1,0)$. The set ST_{n+1} is formed by partitioning each triangle in ST_n into four sub-triangles, using lines joining the midpoints of its three sides, and removing each (open) middle sub-triangle. Alternatively, we can use the three mappings $f_0(x,y) = \left(\frac{2x+1}{4}, \frac{2y+\sqrt{3}}{4}\right)$, $f_1(x,y) = \left(\frac{x}{2}, \frac{y}{2}\right)$, and $f_2(x,y) = \left(\frac{x+1}{2}, \frac{y}{2}\right)$. These mappings are all dilations with ratio $r = \frac{1}{2}$, and each f_i has fixed point v_i for $i \in T$. Starting with the same ST_0 as before, we can set $ST_{n+1} = f_0[ST_n] \cup f_1[ST_n] \cup f_2[ST_n]$, where we write $f[S]$ as an abbreviation for $\{f(x) \mid x \in S\}$. Thus the set ST_{n+1} can be described as the union of three half-scale copies of ST_n. In either case, the Sierpiński triangle is the intersection of all the ST_n, or $ST = \cap_{n=0}^{\infty} ST_n$.

In light of Theorem 3.3 it is natural to enquire about the intersection of the Sierpiński triangle with a magic line. We define the *upper magic line* (UML) as the line joining point $\left(\frac{1}{4}, \frac{\sqrt{3}}{4}\right)$ half way up the left side of ST_0 to the point $\left(\frac{2}{3}, \frac{\sqrt{3}}{3}\right)$ two thirds up the right side, as before. Also, we define the parallel *lower magic line* (LML) as the line connecting the point $(0,0)$ at the lower left corner of ST_0 to the point $\left(\frac{5}{6}, \frac{\sqrt{3}}{6}\right)$ one third up the right side.

Figure 3 shows the amazing results when we intersect the ST_4 approximation of the Sierpiński triangle with the two magic lines. These intersections consist of line segments of two types: *Type 0 segments* that extend from the lower left corner to the point one third of the way up the right side of the solid black subtriangle containing it, and *Type 1 segments* that extend from the midpoint of the left side to the point two thirds of the way up the right side of the solid black subtriangle containing it.

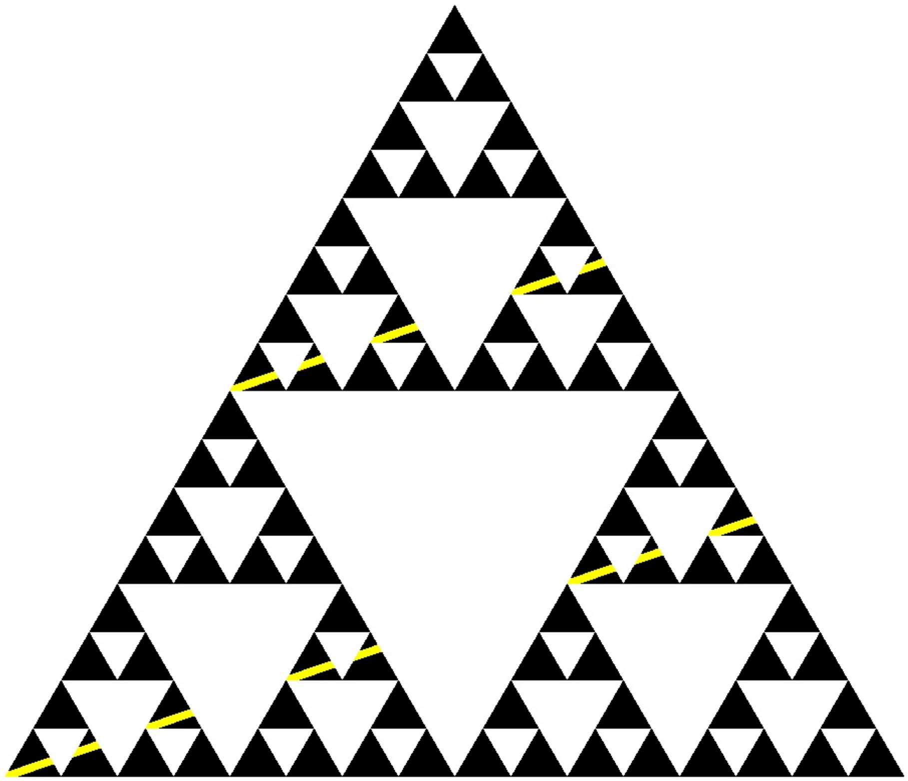

FIGURE 3. The upper and lower magic lines in ST_4.

The intersection $ST_4 \cap UML$ consists of $F_4 = 3$ Type 0 segments and $F_3 = 2$ Type 1 segments, for a total of $F_5 = 5$ segments. The intersection $ST_4 \cap LML$ consists of $F_5 = 5$ Type 0 segments and $F_4 = 3$ Type 1 segments, for a total of $F_6 = 8$ segments. Moreover, the order of the segments of the UML is given by the finite Fibonacci word $W_4 = 01001$, while the order of the segments of the LML is given by $W_5 = 01001010$. We now show that this remarkable pattern continues.

Lemma 4.1. *The following statements are true for all $n \geq 0$.*

(1) *Type 0 segments in ST_n all have length $\frac{L}{2^n}$, and Type 1 segments in ST_n all have length $\frac{L}{2^{n+1}}$, where L is the length of $ST_0 \cap LML$.*
(2) *In passing from ST_n to ST_{n+1} by removing middle triangles, every Type 1 segment in ST_n becomes a Type 0 segment in ST_{n+1}, and every Type 0 segment in ST_n has its third quarter removed, resulting in a Type 0 segment on the left in ST_{n+1} and a Type 1 segment on the right.*
(3) *We have*
   (a) *$ST_n \cap UML = f_0[ST_{n-1} \cap LML]$ and*
   (b) *$ST_n \cap LML = f_1[ST_{n-1} \cap LML] \cup f_2[ST_{n-1} \cap UML]$, both for $n \geq 1$. Therefore,*
   (c) *$ST_n \cap LML = f_1[ST_{n-1} \cap LML] \cup f_2\left[f_0[ST_{n-2} \cap LML]\right]$ for $n \geq 2$.*

Proof. The proof of part (1) is by induction. The length of the Type 0 segment of ST_0 is L by definition, and the length of the Type 1 segment of ST_0 is clearly $\frac{L}{2}$. Moreover, both segment types are half as long in ST_{n+1} as they are in ST_n. Part (2) should be clear from Figure 4. A rigorous proof can be constructed using similar triangles and/or manipulation of coordinates. Part (3) follows immediately from the definitions, and is illustrated in Figure 3. □

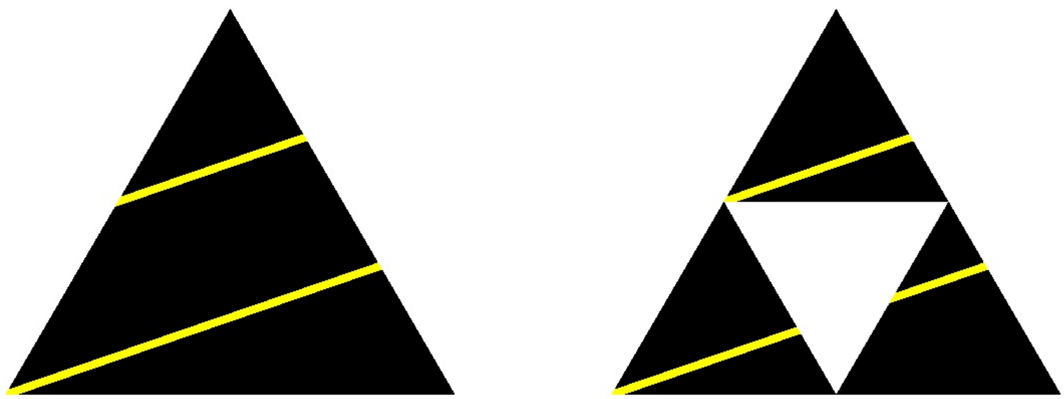

(a) (b)

FIGURE 4. The magic lines intersecting ST_0 (a) and ST_1 (b).

Theorem 4.2. *For every $n \geq 0$, the intersection of the upper magic line with the ST_n approximation of the Sierpiński triangle consists of F_n Type 0 segments and F_{n-1} Type 1 segments, for a total of F_{n+1} segments, ordered according to the finite Fibonacci word W_n. Similarly, the intersection of the lower magic line with the ST_n approximation of the Sierpiński triangle consists of F_{n+1} Type 0 segments and F_n Type 1 segments, for a total of F_{n+2} segments, ordered by the finite Fibonacci word W_{n+1}.*

Proof. The claim is clearly true for $n = 0$ and $n = 1$, provided we extend the definition of Fibonacci number to include $F_{-1} = 1$. Also, from Lemma 4.1 part (2), we see that the line segments of each magic line satisfy the morphism φ in the first characterization of the finite Fibonacci words. Alternatively, from Lemma 4.1 part (3)(c), we see that the line segments of the LML satisfy the concatenation characterization of the finite Fibonacci words. The result for the UML then follows from Lemma 4.1, part (3)(a). □

5. The Fibonacci Fractal

Just as the sets ST_n approach the Sierpiński triangle, a fractal of Hausdorff dimension $\log_2(3)$, the sets $ST_n \cap LML$ approach a fractal of smaller dimension. In this section we explore this fractal. Our exploration mimics the usual treatment of the well known Cantor set, or the Cantor middle-third set, by starting with a closed line segment and systematically removing open subsets. We use the length L from Section 4 as our new unit of length, refer to Type 0 segments as *long segments* and Type 1 segments as *short segments*, and invoke Lemma 4.1, part (2) in our construction.

We start with set $FF_0 = [0, 1]$, the closed unit interval, which we define to be a long segment. There are two rules for forming FF_{n+1} from FF_n:

(1) Each short segment of FF_n remains intact, but becomes a long segment in FF_{n+1}.
(2) The (open) third quarter of each long segment of FF_n is removed, leaving a long segment on the left and a short segment on the right in FF_{n+1}.

Thus, for example, we have $FF_1 = \left[0, \frac{1}{2}\right] \cup \left[\frac{3}{4}, 1\right]$ and $FF_2 = \left[0, \frac{1}{4}\right] \cup \left[\frac{3}{8}, \frac{1}{2}\right] \cup \left[\frac{3}{4}, 1\right]$. The *Fibonacci fractal* is the intersection of these sets, or $FF = \cap_{n=0}^{\infty} FF_n$. We observe that being the intersection of closed sets, the Fibonacci fractal is closed, and as it is also bounded, it is a compact subset of $\mathbb{R}$.

We display the Fibonacci fractal in Figure 5 in a manner often used to display the Cantor set. The top bar represents the set FF_0, and successive rows represent the successive approximations FF_n for $1 \leq n \leq 8$.

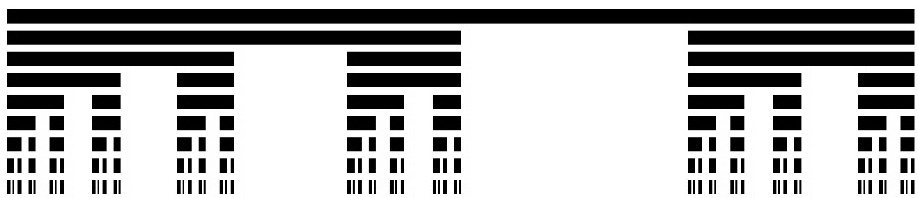

FIGURE 5. Approximations FF_0 to FF_8 of the Fibonacci fractal.

The following theorem is essentially a recasting of parts of Theorem 4.2 and Lemma 4.1 part (a).

Theorem 5.1. *For every $n \geq 0$, the FF_n approximation of the Fibonacci fractal consists of F_{n+1} long segments, each of length $\frac{1}{2^n}$, and F_n short segments, each of length $\frac{1}{2^{n+1}}$, for a total of F_{n+2} segments. The total length of these segments is $\frac{F_{n+1}}{2^n} + \frac{F_n}{2^{n+1}} = \frac{F_{n+3}}{2^{n+1}}$, which approaches a limit of 0 as n increases. Representing a long segment by 0 and a short segment by 1, these segments are ordered by the finite Fibonacci word W_{n+1}.*

An alternative approach to the Fibonacci fractal is through mappings $g_1(x) = \frac{x}{2}$ and $g_2(x) = \frac{x+3}{4}$. Mapping g_1 is a dilation with ratio $\frac{1}{2}$ and fixed point 0, sending the unit interval onto the interval $\left[0, \frac{1}{2}\right]$. Mapping g_2 is a dilation with ratio $\frac{1}{4}$ and fixed point 1, sending the unit interval onto the interval $\left[\frac{3}{4}, 1\right]$.

Theorem 5.2. *For all $n \geq 2$ we have*

$$FF_n = g_1[FF_{n-1}] \cup g_2[FF_{n-2}].$$

Moreover, in the limit we have

$$FF = g_1[FF] \cup g_2[FF].$$

Proof. We have

$$g_1\left[FF_1\right] = g_1\left[\left[0, \tfrac{1}{2}\right] \cup \left[\tfrac{3}{4}, 1\right]\right] = \left[0, \tfrac{1}{4}\right] \cup \left[\tfrac{3}{8}, \tfrac{1}{2}\right]$$

and

$$g_2\left[FF_0\right] = g_2\left[[0, 1]\right] = \left[\tfrac{3}{4}, 1\right]$$

so

$$FF_2 = \left[0, \tfrac{1}{4}\right] \cup \left[\tfrac{3}{8}, \tfrac{1}{2}\right] \cup \left[\tfrac{3}{4}, 1\right] = g_1\left[FF_1\right] \cup g_2\left[FF_0\right]$$

and the first claim is true for $n = 2$. The truth of this claim for larger n follows by induction.

For the second claim we have

$$\begin{aligned} x \in FF &\Leftrightarrow x \in FF_n \text{ for all } n \geq 2 \\ &\Leftrightarrow x \in g_1[FF_{n-1}] \cup g_2[FF_{n-2}] \text{ for all } n \geq 2 \\ &\Leftrightarrow x \in g_1[FF_n] \text{ for all } n \geq 1, \text{ or } x \in g_2[FF_n] \text{ for all } n \geq 0 \\ &\Leftrightarrow x \in g_1[FF] \cup g_2[FF]. \end{aligned}$$ □

We can use Theorem 5.2 to derive the Hausdorff dimension of the Fibonacci fractal following, for example, the methods explained in Edgar [5].

Corollary 5.3. *The Fibonacci fractal has Hausdorff dimension* $\log_2(\phi)$*, where* ϕ *is the Golden ratio* $\frac{1+\sqrt{5}}{2}$*, the limiting ratio of consecutive Fibonacci numbers* $\frac{F_{n+1}}{F_n}$*.*

Proof. We have seen that $\{g_1, g_2\}$ is a contracting iterated function system with invariant set FF and ratio list $\left(\frac{1}{2}, \frac{1}{4}\right)$. The similarity dimension of the system is then $\log_2(\phi)$, the unique nonnegative number s satisfying the equation $\left(\frac{1}{2}\right)^s + \left(\frac{1}{4}\right)^s = 1$ (cf. [5, Theorem 4.1.1]). The open interval $(0, 1)$ satisfies Moran's open set condition for this iterated function system, which implies that $\log_2(\phi)$ is also the Hausdorff dimension of the Fibonacci fractal (cf. [5, Theorem 6.5.4]). □

It is well known that the Cantor set is the set of numbers in $[0, 1]$ that can be written in base 3 using only the ternary digits 0 and 2. A somewhat similar but more complicated characterization exists for numbers in the Fibonacci fractal.

Theorem 5.4. *A number* x *with* $0 \leq x \leq 1$ *is in the Fibonacci fractal if and only if* x *can be written in binary using the binary digit 0 and pairs* 11 *of the binary digit* 1*. Equivalently,* x *is not in the Fibonacci fractal if and only if every binary representation of* x *contains at least one odd length block of the binary digit* 1*.*

Proof. We in fact prove that a number x is removed when forming FF_n if and only if every binary representation of x begins after the radix point with a string of length $n-1$ made up of copies of the bit 0 and pairs 11 of the bit 1, followed by the bit 1, followed by the bit 0. The first odd length block of 1 bits will then end with the 1 in position n.

The proof is by induction. There are no numbers removed in forming FF_0 and no numbers satisfy the characterization, so the claim is true for $n = 0$. The numbers removed when forming FF_1 are those for which $\frac{1}{2} < x < \frac{3}{4}$, i.e., those in the third quarter of FF_0. The binary representation of each of these numbers must start $0.10b_3b_4\ldots$, as claimed. Moreover, the numbers that have a representation of this form are those for which $\frac{1}{2} \leq x \leq \frac{3}{4}$. However, the endpoints have alternative representations, $\frac{1}{2} = 0.0111\ldots$ and $\frac{3}{4} = 0.110000\ldots$, and are not removed. The claim is thus true for $n = 1$.

Now suppose the claim is true for all numbers removed prior to the forming of FF_n, for some $n \geq 2$. The numbers that are removed in forming FF_n are exactly the images under g_1 of the numbers removed in forming FF_{n-1}, together with the images under g_2 of the numbers removed in forming FF_{n-2}. Now for any number $x = (0.b_1b_2b_3\ldots)_{(2)}$, we have $f_1(x) = (0.0b_1b_2b_3\ldots)_{(2)}$ and $f_2(x) = (0.11b_1b_2b_3\ldots)_{(2)}$. Invoking the inductive hypothesis for x in FF_{n-1} and x in FF_{n-2}, we obtain the desired result. □

For example, the numbers $\frac{4}{7} = (0.100\overline{100})_{(2)}$ and $\frac{5}{7} = (0.101\overline{101})_{(2)}$ are both removed in forming FF_1, the number $\frac{2}{7} = (0.010\overline{010})_{(2)}$ is removed in forming FF_2, and the number

$\frac{1}{7} = (0.001\overline{001})_{(2)}$ is removed in forming FF_3. The numbers $\frac{3}{7} = (0.011\overline{011})_{(2)}$ and $\frac{6}{7} = (0.110\overline{110})_{(2)}$ remain in FF, even though neither one is an endpoint of a removed interval.

Corollary 5.5. *The Fibonacci fractal contains an uncountable number of points.*

Proof. For any x from 0 to 1, replace each 1 bit in the binary representation of x with 11. The result will be a point in FF. Moreover, it is easy to show that every member of FF has a unique binary representation of this form. □

The Fibonacci fractal was mentioned briefly in two earlier works, where it was called the asymmetric Cantor set. It was introduced by Farmer [6], with a somewhat different construction, as an example of a set with information dimension different from Hausdorff dimension. Unfortunately the value given for the Hausdorff dimension is wrong. This error was pointed out and corrected by Tsang [9]. The construction used in those papers removes the third quarter of all segments, not just the long ones. It therefore does not display the finite Fibonacci words, and misses the rich Fibonacci aspects of our construction.

6. Ongoing Work

We are currently extending our work in two directions. First, we are looking at graphs other than the graphs H_3^n. For example, the graphs S_4^n, discussed in [7, Section 4.2], are a natural extension of the Hanoi graphs and have a standard embedding into tetrahedra in $\mathbb{R}^3$. Vertices twice as far from one corner vertex as from another in S_4^n lie in a *magic plane* and are counted by the Pell numbers.

We are also looking at multiples other than $m = 2$ in defining key vertices as those with $d_2 = m \cdot d_0$. For $m = 5$, for example, we can show that the number of these key vertices in H_3^n is 0 if n is odd, and F_{k-1} when $n = 2k$.

References

[1] J.-P. Allouche and J. Shallit, *Automatic Sequences*, Cambridge University Press, Cambridge, 2003.

[2] J Bennish, *The Tower of Hanoi problem and mathematical thinking*, Missouri J. Math. Sci., **11** (1999), 164–166.

[3] N. Claus (= É. Lucas), *La Tour d'Hanoï, Véritable casse-tête annamite*, P. Bousrez, Tours, 1883.

[4] N. Claus (= É. Lucas), *La Tour d'Hanoï, Jeu de calcul*, Science et Nature, **1** (1884) 127–128.

[5] G. Edgar, *Measure, Topology, and Fractal Geometry*, Second Edition, Springer, New York, 2008.

[6] J. D. Farmer, *Information dimension and the probabilistic structure of chaos*, Z. Naturforsch., **37a** (1982), 1304–1325.

[7] A. M. Hinz, S. Klavžar, and C. Petr, *The Tower of Hanoi — Myths and Maths*, Second Edition, Birkhäuser, Cham (Switzerland), 2018.

[8] OEIS Foundation Inc. (2011), The On-Line Encyclopedia of Integer Sequences, http://oeis.org. Accessed September 30, 2018.

[9] K. Y. Tsang, *Dimensionality of strange attractors determined analytically*, Phys. Rev. Lett., **57** (1986), 1390–1393.

MSC2010: 00A08, 05C12, 11B39, 28A80, 68R15

Department of Mathematics, LMU München, Munich, Bavaria, Germany
E-mail address: hinz@math.lmu.de

Department of Computer Science, The College of William & Mary, Williamsburg, Virginia, U.S.A.
E-mail address: stockmeyer@cs.wm.edu